

Structure and Properties of a Polypropylene Containing Random Ethylene Units Modified with a Hydrogenated Hydrocarbon Resin

Sossio Cimmino,* Donatella Duraccio, Clara Silvestre

Summary: The system formed by a polypropylene containing random low ethylene content (EP copolymer) of and a hydrogenated hydrocarbon resin (HR) is investigated in order to study the influence of resin (up to 20% in wt) on properties of blends and derived films. The random EP copolymer used is MoplenEP2C37F and the resin is MBG273 of Hercules Chemical Co. DSC and DMTA analyses of the blends show increase of T_g with resin content indicating that the two components are compatible in the amorphous phase. WAXD spectra show that MBG273 influences slightly the crystalline structure of EP copolymer. In fact the diffractograms of the EP copolymer and 95/5 blend present, beside the predominant peak of α form, also a small span denoting presence of γ form; this span is not detectable on spectra of 90/10 and 80/20 samples. The crystallization during the cooling is found to be only lightly delayed by the HR: in fact, only 4 degrees is the difference between the T_c values of EP copolymer and 80/20 blend. Stress-strain test performed at room temperature show that MBG273 induces increase of Young's modulus and small decrease of elongation at break as function of resin content. An important effect is on the water vapour permeability, which decreases with resin content. The permeability and tensile properties are related to the increase of the glass transition with the addition of MBG273 that transforms gradually the amorphous of the material from rubbery to glassy. The results reported in this work indicate that an addition of 5–10% of MBG273 changes favourably properties, as Young's modulus and water vapour permeability, of an EP copolymer designed for the production of films for packaging application.

Keywords: blend; film; hydrogenated hydrocarbon resins; mechanical properties; polypropylene; propylene-ethylene random copolymer

Introduction

The modification of isotactic polypropylene (iPP) with low molecular weight resins, to obtain film to be used in the packaging sector, is one of the tasks that researchers and industrial groups are carrying on since several years. Low molecular weight resins are added to cause drastic modification in the structure and morphology of iPP.^[1–12] Depending on the nature of the resin and

film preparation, the final film can be characterized by a higher elastic modulus, improved optical properties, lower permeability to gases, water vapour and aromas, and lower melt viscosity, compared to pure iPP film.^[1,9,12] Besides these numerous positive effects on iPP, the resin can delay the crystallization of iPP during the production of films from the melt (by cast or blowing) with the consequence that the crystallization is not complete. The completion of the crystallization (known as post crystallization phenomenon) can occur during the storage with the consequence that films stick together with great damage for the sale. In reference 12 it is reported

Istituto di Chimica e Tecnologia dei Polimeri - C.N.R.
Via Campi Flegrei, 34, 80074, Pozzuoli (NA), Italy
E-mail: cimmino@ict.cnr.it

great positive effects of MBG273 on mechanical properties of an iPP (namely MoplenX30S), but also the effect to delay the crystallization. In a paper in preparation it is shown how the post crystallization phenomenon is resolved with the addition of a third component, incompatible with iPP, to complete the crystallization during the cooling from the melt.^[13]

In the polypropylene family, polypropylenes containing random 1-olefin units are becoming an important class of plastic materials. They contain, along their backbone, comonomeric units of 1-olefin (as ethylene, 1-butene) randomly distributed. The presence of the co-monomer units and their distribution in the backbone of iPP molecules changes greatly the properties as molecular weight and isotacticity are modified. The introduction of the second comonomer along with propylene segments promotes the formation of shorter stereo regular blocks, which melt at a lower temperature. The physical properties of these copolymers depend also on the degree of crystallinity, structure and overall morphology that are defined by crystallization conditions. A satisfying balance of clarity, flexibility, and mechanical strength, a higher resiliency and resistance to mechanical solicitation than iPP make them particularly suitable for the packaging industry. These copolymers are also characterized by lower heat-sealing temperatures, which allow faster and more economic processing. This property is related to the lower melting temperature due to the insertion of the comonomer along the polymer chain.

The effect of copolymerization on the formation of the several crystalline phases of iPP was studied by Mezghani and Phillips.^[14,15] It was found that copolymerization causes the formation of the γ form of iPP at atmospheric pressure in high molecular mass sample isothermally crystallized at low under-cooling, whereas for the homopolymer the γ form can be obtained by crystallization at elevated pressure or by crystallization at atmospheric pressure of low molecular fractions.

Later, Dimiska and Phillips^[16] investigated the influence of the ethylene content and tacticity on crystallinity, T_m and heat of fusion of several EP copolymers with ethylene content between 2.6 and 15.6. The results were accounted for by hypothesizing a partial inclusion of ethylene units in PP crystals.

In a recent work, the polymorphism behaviour, crystallization and the overall morphology of an EP copolymer containing 2% ethylene sequences (MoplenEP1X35F) with respect to the crystallization conditions have been investigated.^[17] The study showed that EP copolymer can present different modifications and morphologies by changing crystallization and annealing conditions. In particular it was found that the presence of ethylene sequences reduces the spherulite growth rate at a given T_c . The decrease was related not only to the rejection of ethylene sequences from the crystallization growth front, but also to the formation of different crystals presenting different crystallization kinetics.

This work continues the study of EP copolymer with the particular objective to acquire scientific knowledge of systems formed by MoplenEP2C37F and a petroleum hydrogenated hydrocarbon resin (HR) to produce blends suitable for the production of films for packaging. For this work it was chosen MoplenEP2C37F, at place of MoplenEP1X35F used in reference 17, because it is particularly indicated for the production of films for packaging application.

Hydrogenated hydrocarbon resin derives from a mixture of unsaturated monomers obtained as volatile by-products of naphtha. The resin has water resistance, wide compatibility with other resins, chemical neutrality and good electrical properties.^[12,18] Hydrogenated hydrocarbon resins are non-toxic and non-sensitizing to the skin and their use in polymeric and resinous coatings for containers that come in contact with food for human consumption is regulated by the Food and Drug Administration of the U.S. Department of Health Education and Welfare.

Experimental

Materials

The materials used are a slightly modified polypropylene random copolymer with 3.1 wt% ethylene sequences produced by Basell [MoplenEP2C37F: weight-average molecular weight (M_w) = $5.29 \cdot 10^5$ g/mol, number-average molecular weight (M_n) = $3.3 \cdot 10^4$, melt flow index (M.F.I.) (230 °C, 2.16 kg) = 6 g/10 min, density = 0.9 g/cm³]; and a hydrogenated hydrocarbon resin, MBG273, produced by Eastman Chemical Company (M_w = $1.47 \cdot 10^3$ g/mol, M_n = $9.0 \cdot 10^2$ g/mol, M_z = $2.4 \cdot 10^3$ g/mol). The glass transition temperature (T_g), determined by differential scanning calorimetric (DSC), was detected at 87 °C.

Resin MBG273 is an oligomer obtained in three steps: polymerization of monomers such as styrene, α -methyl-styrene, vinyl-toluene, cyclopentadiene and indene to form the aromatic precursor resin; weak hydrogenation reaction to saturate the backbone along the chain; strong hydrogenation reaction to destroy the aromaticity of ring and to create a fully alicyclic resin.

Trough the paper “MoplenEP2” and “EP2” stand for MoplenEP2C37F, whereas “HR” for the resin MBG273.

Blend Preparation

MoplenEP2 and HR components were mixed in a Brabender-like apparatus (Rheocord EC of HAAKE Inc.) at 190 °C and 32 rpm for 10 minutes. The blends compositions were 100/0, 95/5, 90/10, 80/20 (wt/wt).

Preparation of Compression-Molded Samples

The mixed material was compression-moulded in a press at 190 °C for 3 minutes without applied pressure to allow complete melting and for other 3 minutes with the pressure raised to 20 MPa. Then the plates of the press, fitted with cooling coils, were rapidly cooled to room temperature by using cold water. Finally the pressure was released and the mould, with a rectangular

shape and dimension of 70 × 110 mm, removed from the plates. These samples, 1 mm thick, were used for the DSC, DMTA and tensile tests.

Preparation of Films

Films with thickness of 120 μ m, for WAXD and permeability measurements, were obtained by using the same procedure utilized for the compression-moulded samples but with pressure at 40 MPa.

Wide-Angle X-ray Diffraction (WAXD)

Measurements

WAXD measurements were carried out at room temperature with a Philips PW 1050 power diffractometer (with CuNi-filtered radiation) equipped with a rotating sample holder device. The WAXD experiments were performed to detect influence of HR on the structure of the Moplen EP2.

Thermal Analysis

The calorimetric properties of the compression-moulded blends were investigated with a differential scanning calorimeter (Mettler DSC822). The apparatus was calibrated with pure indium at various scanning rates. About 10 mg of the sample was heated from –80 to 200 °C at a rate of 20 °C/min. The observed melting temperature (T_m) was obtained from the maxima of the endothermic peaks. The glass transition temperature (T_g) was determined at the maximum of the peak obtained by applying the first derivative procedure. The crystallinity indices of the MoplenEP2 phase [$X_c(\text{MoplenEP2})$] and of overall blend [$X_c(\text{blend})$], were calculated from:

$$X_c(\text{MoplenEP2})$$

$$= \Delta H * (\text{MoplenEP2}) / \Delta H^\circ(\text{ipp})$$

$$X_c(\text{blend}) = \Delta H * (\text{blend}) / \Delta H^\circ(\text{ipp})$$

where $\Delta H^\circ(\text{ipp})$ is the enthalpy of melting per gram of 100% crystalline iPP (210 J g^{–1}) and $\Delta H^*(\text{MoplenEP2})$ and $\Delta H^*(\text{blend})$ the measured enthalpy of melting.

Non isothermal crystallization of the samples was investigated by following this procedure: each sample was heated from 25

to 200 °C, kept at this temperature for 4 minutes and then cooled to room temperature at 3 rates (5, 10 and 20 °C/min).

DMTA

Dynamic mechanical data were collected at 1 Hz and at heating rate 3 °C/min from –80 to 110 °C under nitrogen atmosphere with a Dynamic Mechanical Thermal Analyser MK III, Polymer Laboratories, configured for automatic data acquisition. The experiments were performed in bending mode. Two tests for each composition were performed. The two tests gave the same results.

Tensile Tests

Dumbbell-shaped specimens were cut from 1 mm thick sheets and used for the tensile measurements. Stress-strain curves were obtained using an Instron machine (Model 4505) at room temperature (~25 °C) at a crosshead speed of 5 mm/min. Young's modulus, stress and strain at yield and at break points were calculated from 10 tests performed for each composition.

Water Vapour Permeability

Water vapour permeability test was conducted according to ASTM E96 for the water method. The instrumental apparatus is a Multiperm Extra Solution. It consists of a double chamber diffusion cell. The film is inserted between the two chambers: a nitrogen flux with water vapour enters in the lower one and a nitrogen flux enters in the upper one. The water vapour diffusion through the film is measured by a zirconium oxide sensor. The area of the film involved in the experiment is = 50 cm². Collected data are converted in water vapour transmission rate (WVTR) that is defined as the steady vapour flow in time through an area of a body, normal to specific parallel surfaces, under specific conditions of temperature and humidity at each surface. Measurement were carried out by using "tropical conditions" that are 90% of U.R. and 38 °C. Sensitivity reaches 10^{–17} ppm H₂O.

The results are reported in water vapour permeability that is the time rate of water

vapour transmission through the area of a flat material of a certain thickness induced by a vapour pressure difference between two specific surfaces. Three experiments for each sample composition were performed.

Results

WAXD

The X-ray power diffraction profiles of MoplenEP2 and blends are shown in Figure 1. It is recalled that iPP can present several crystalline forms, as α , β , γ and smectic.^[19,20] The presence of α form is revealed by the peak at $2\theta = 18$ –19° on the diffraction pattern, whereas γ form is detectable by the peak at $2\theta = 19.2$ –20.5°. The α form is that generally present in iPP obtained from cooling or quenching from the melt. The γ phase is obtainable for high Mw by crystallization at elevated pressure. The γ phase can be obtained at atmospheric pressure only for low molecular weight material. Turner-Jones et al.,^[21,22] Mezghani and Phillips,^[14,15] and Silvestre et al.^[17] have reported that the γ phase can be formed at atmospheric pressure also for high molecular weights in the case of

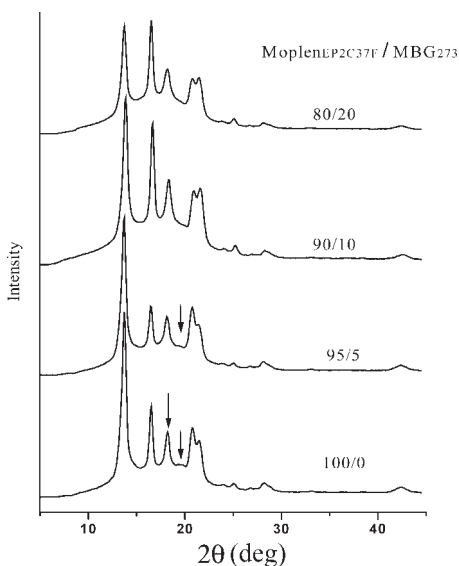


Figure 1. WAXD profiles of MoplenEP2/HR blends.

slightly modified PP random copolymers isothermally crystallized at low undercooling or crystallized with very slow cooling rate from the melt. The diffractograms of all the samples in Figure 1 show presence of a strong diffraction peak at $2\theta = 18.6^\circ$ indicating that in these samples the polypropylene is basically in α form. The diffractograms of MoplenEP2 and 95/5 sample presents also a tiny span at about $2\theta = 19.3^\circ$ revealing that a small amount of crystals exists in γ form.

DSC Analysis. Thermo-analytical curves of MoplenEP2 and its blends with MBG 273 are reported in Figure 2a. The thermograms present one endothermic peak due to the melting of monoclinic crystals of polypropylene. The observed melting point (T_m) and the crystallinity index (X_c) are reported in Table 1. It is found that T_m decreases slightly with HR content. T_m of MoplenEP2, in fact, is read

Table 1.

Melting point, Crystallization Index of MoplenEP2/MBG273 blends.

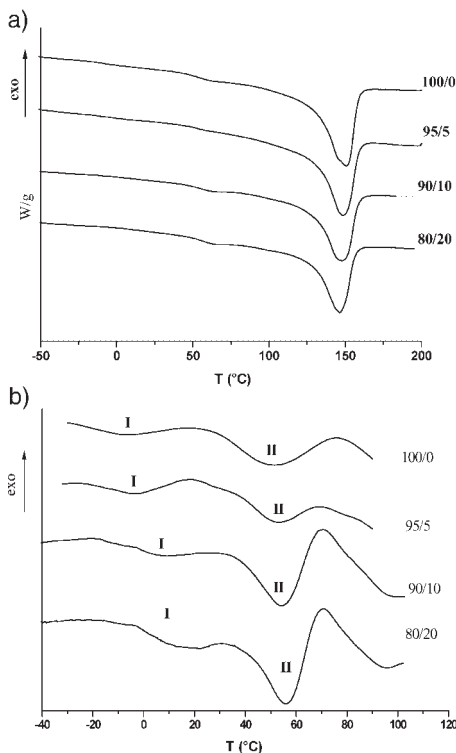
MoplenEP2/ MBG273	T_m	X_c (blend)	X_c (MoplenEP2)
(wt/wt)	($\pm 1^\circ\text{C}$)	(%)	(%)
100/0	151	40 ± 2	40 ± 2
95/5	149	41 ± 2	43 ± 2
90/10	148	35 ± 2	39 ± 2
80/20	146	33 ± 2	41 ± 2

at 151°C whereas the value of 80/20 blend is at 146°C . This decrease will be commented below. X_c referred to MoplenEP2 content in the blend (see fourth column of Table 1) is constant with composition, that is, in each blend the percentage of crystallized MoplenEP2 is the same, about 40%.

To investigate the influence of the resin on the T_g of MoplenEP2, first derivatives of thermo-analytical curves from -40 to 100°C were performed and reported in Figure 2b.

It is recalled that semicrystalline polymers present two glass transitions, named as $T_g(L)$ and $T_g(U)$.^[23–27] $T_g(L)$ arises from the main amorphous molecules; $T_g(U)$ arises from the amorphous material under restrains by crystals, that is, from relaxation of the molecules or sections of molecules interconnected to the crystalline phase, as short cilia, loose loops and tie molecules. The first derivative curves on Figures 2b show the presence of two peaks, labelled as I and II, corresponding to lower glass transition $T_g(L)$ and upper glass transition $T_g(U)$.^[12,23,24] MoplenEP2 presents the first peak with maximum [taken as $T_g(L)$] at about -6°C ; the second peak, $T_g(U)$, evolves in the range from 30 – 70°C , with a maximum at about 52°C .

For the blends, $T_g(L)$ increases with HR content. These results indicate complete compatibility of HR with the amorphous phase of MoplenEP2. If the resin were phase separated from amorphous MoplenEP2, the thermo-analytical curve would have presented a transition at about the T_g of the hydrocarbon resin as it is shown with the following experiment. 6.9 mg of copolymer and 1.7 mg of HR were put in the

**Figure 2.**

(a) DSC thermograms of MoplenEP2/MBG273 blends
(b) First derivative of DSC thermograms of blends.

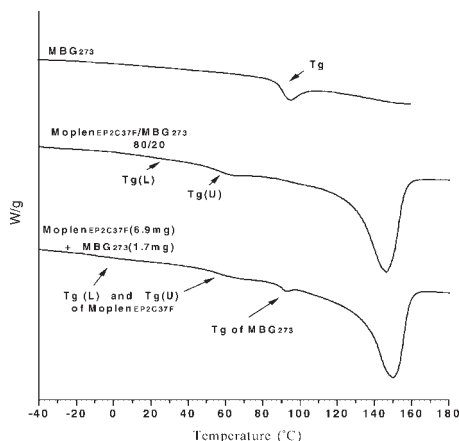


Figure 3.

Thermo-analytical curves of MBG273 resin, 80/20 blend (mixed components) and physical 80/20 blend.

same DSC pan to reproduce a virtual 80/20 blend, named as physical blend, that is, a blend with components completely phase separated. The thermo-analytical curve of this physical blend is reported in Figure 3 and compared to the curves of 80/20 blend and MBG273. The curve of the physical blend shows two peaks, at -8 and 56°C corresponding to T_g (L) and T_g (U) of MoplenEP2 respectively, and a third peak due to the T_g of MBG273 (87°C).

Passing to the analysis of peaks (II) of Figure 2b it is observed that only T_g (U) of 80/20 blend seems to be slightly influenced by the hydrocarbon resin. Its maximum, in fact, is only at 4 degrees higher than peak (II) of MoplenEP2. This point deserves a future investigation because if HR is compatible with the amorphous generating T_g (L), there is no plausible reason that it should not have similar effect also on the amorphous generating T_g (U).

As cited above, T_m decreases with the resins. The decrease of the melting point of a semicrystalline polymer with the addition of a second component can be due to two factors: kinetic effect and thermodynamic effect.^[28,29] The increase of T_g (L) of blends found by DSC (confirmed also by DMTA, see below) has been accounted for by compatibility between the two components, so it can be affirmed that the decrease of

T_m observed is due to thermodynamic effect. Of course contributions of the kinetic effect cannot be excluded.

The enterprises producing films from pellets require that the crystallization of the film (either by blowing or cast methods) must be fast and complete, in order to avoid, during the storage, changes of morphology and/or further crystallization process which cause films to stick together. So the addition of second components must not influence negatively too much the crystallization rate. In order to determine the influence of the resin on the crystallization of MoplenEP2, non-isothermal crystallization experiments were performed as function of composition and cooling rate. Thermo-analytical curves were obtained during the cooling from melt (200°C) at three rates (5 , 10 and $20^{\circ}\text{C}/\text{min}$).

Figure 4 reports the cooling curves at $20^{\circ}\text{C}/\text{min}$ as function of composition. Table 3 reports the onset temperature (T_0) and the temperature corresponding to the maximum of the crystallization peaks (T_c). It emerges that the lower is the heating rate the higher is the temperature of the crystallization peaks. Therefore, at low heating rate, a lower under-cooling is needed to crystallize. It is found, moreover, that for concentration of interest for industries (generally from 5 to 10%) the resin does not decrease significantly the crystallization temperature. In fact, for example, at cooling rate of $20^{\circ}\text{C}/\text{min}$, T_c of MoplenEP2 is 96°C and the values for 95/5 and 90/10 blends are only 4 degrees lower, 92°C . Finally, we can also exclude post crystallization phenomenon for the blends since DSC performed on blends, cooled very fast from the melt, present percentage of

Table 2.

Glass transitions temperatures of MoplenEP2/MBG273 blends.

MoplenEP2/MBG273	T_g (L)	T_g (U)
(wt/wt)	($\pm 2^{\circ}\text{C}$)	($\pm 2^{\circ}\text{C}$)
100/0	-6	52
95/5	-3	53
90/10	9	54
80/20	in the range 12 – 20	56

Table 3.

Crystallization properties of MoplenEP2/MBG273 blends at different heating rates.

MoplenEP2/MBG273 (wt/wt)	5 °C/min		10 °C/min		20 °C/min	
	T_o	T_c	T_o	T_c	T_o	T_c
	(± 1 °C)	(± 1 °C)	(± 1 °C)	(± 1 °C)	(± 1 °C)	(± 1 °C)
100/0	113	105	110	101	107	96
95/5	110	102	109	98	104	92
90/10	109	101	107	96	104	92
80/20	109	98	106	93	98	88

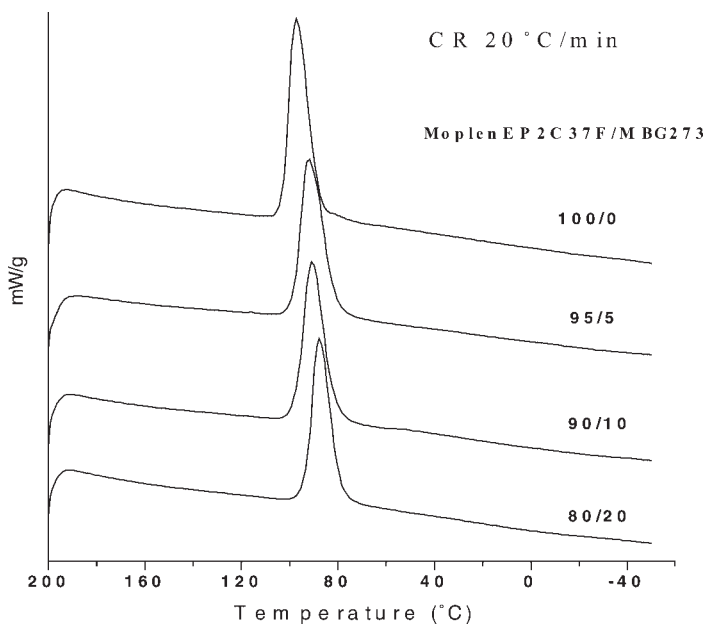
crystallinity referred to MoplenEP2 equal to that of plain polyolefin, as those reported in the fourth column in Table 1.

DMTA Analysis

The curves of $\tan\delta$ are reported in Figure 5. $\tan\delta$ curve of MoplenEP2 presents a first peak with a maximum at about 10 °C and a second peak, very broad, extending from circa 50 to over 100 °C. Peak (I) is due to the main glass transition, $T_g(L)$, and peak (II) is due to the secondary transition $T_g(U)$. The addition of HR to MoplenEP2 increases T_g of the blends and hence peak (I) shifts to higher temperatures. For 5 and 10% compositions, peak (I) is still distinguishable from peak (II). For 80/20 sample

the increase of $T_g(L)$ is such that it merges with peak II forming one broad peak. From the analyses of the curves it cannot be deduced if there is any influence of the resin on $T_g(U)$.

The storage modulus, E' , is reported in Figure 6a. In order to analyze E' curves it is convenient to divide the figure in three regions. In the first region, extending from -80 °C to $T_g(L)$, the amorphous phase is in glassy state and the storage modulus is constant up to the T_g value that increases with MBG273 content. In fact the plateau of E' for 80/20 blend is longer than that of MoplenEP2. Another effect of the resin in this region, even if very small, is that the value of E' increases along the series from

**Figure 4.**

Crystallization curves during cooling at 20 °C/min of MoplenEP2/MBG273 blends.

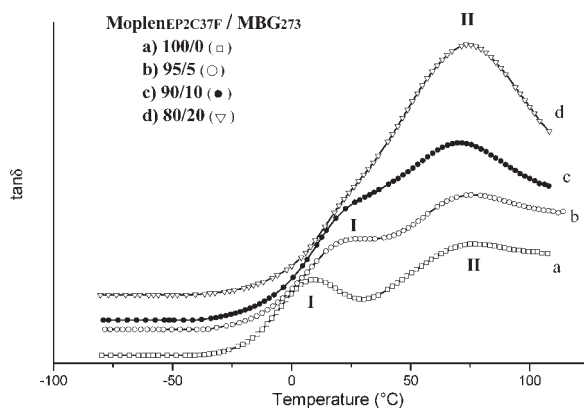


Figure 5.

Tan δ of MoplenEP2/MBG273 blends.

100/0 to 80/20. In the second region, from T_g(L) to about 50 °C, E' decreases slightly with T: the amorphous is changing from glassy to rubbery, passing through a leathery state. In the third region, above 50 °C, there is an inversion of the position of

E' curves: the storage modulus is lower for blends with higher resin content. In this region, the transformation of the amorphous in rubbery state is complete and the main contribution to the modulus is given by a crystalline phase that is highest for

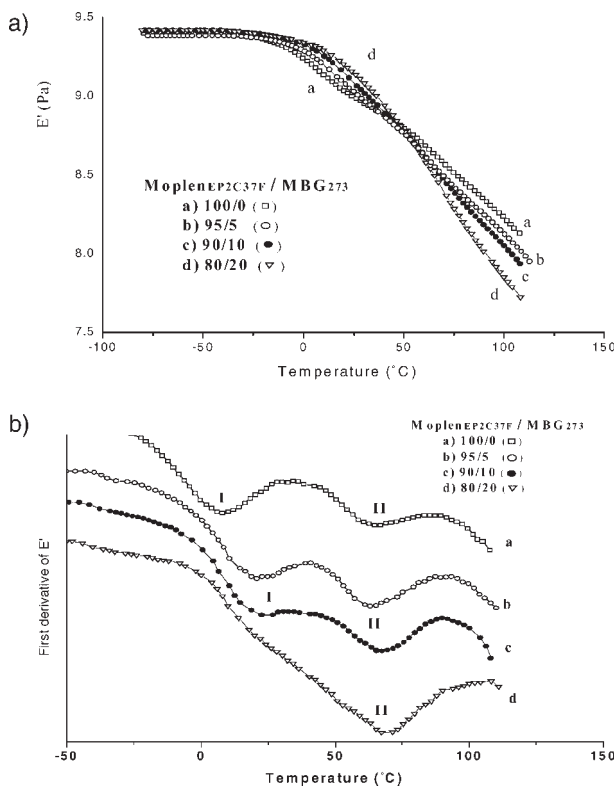


Figure 6.

(a) Storage modulus, E', of MoplenEP2/HR blends (b) First derivative of storage modulus, E', of Figure 6a.

plain MoplenEP2 and lowest for 80/20 blend.

Figure 6b shows the first derivative E' curves. It is worth to note that first derivative curves are equivalent to $\tan\delta$ curves in Figure 5 and similar to the first derivative curves of DSC in Figure 1b. Peak (I) corresponds to the first inflection point of the curve in Figure 6a and represents $T_g(L)$. Peak (II) corresponds to the second inflection point due to $T_g(U)$. The shift of Peak (I) at higher temperature once again indicates the increase of $T_g(L)$ with MBG273 resin. Peak (II) results very slightly shifted at higher T . In fact, as already found for the first derivatives of DSC curves (Figure 1b), the maximum of the peak (II) of the 80/20 sample results 4 degrees higher than that of MoplenEP2 sample.

From the results obtained by DSC and DMTA, it can be deduced that HR MBG273 is compatible with amorphous MoplenEP2 at the three compositions investigated here. The presence of a single T_g dependent on composition indicates that the compatibility is at level of molecular segments.

Tensile Properties

Tensile properties determined at room temperature and at crosshead speed of

5 mm/min are shown in Figure 7. All the samples show stress-strain behaviour typical of ductile semicrystalline polymers, with yield point, cold-drawing and fibre formation region. Modulus of Young (E), stress at yield (σ_y), strain at yield (ε_y), stress at break (σ_b), and strain at break (ε_b) are reported in Table 4.

The Young's modulus, E , increases with the resins content: from 1000MPa for MoplenEP2 to 1245MPa for the material with 20% of HR. Stress and strain at break (σ_b and ε_b) decrease with resin content whereas stress and strain at yielding (σ_y and ε_y) result independent of composition, except ε_y of 80/20 blend.

The tensile behaviours are interpreted as follows: at room temperature (RT) the amorphous phase of MoplenEP2 is in the rubbery state, because $RT > T_g(L)$; the addition of MBG273 to MoplenEP2 changes gradually the physical state of amorphous phase from rubbery to a glassy phase, because the $T_g(L)$ increases to higher values depending on composition. The amorphous of the system becomes harder with the resin. The value of E depends on two factors: the overall crystallinity and the physical state of the amorphous phase. The decrease of the overall crystallinity with HR content has the effect to reduce the modulus E , whereas the

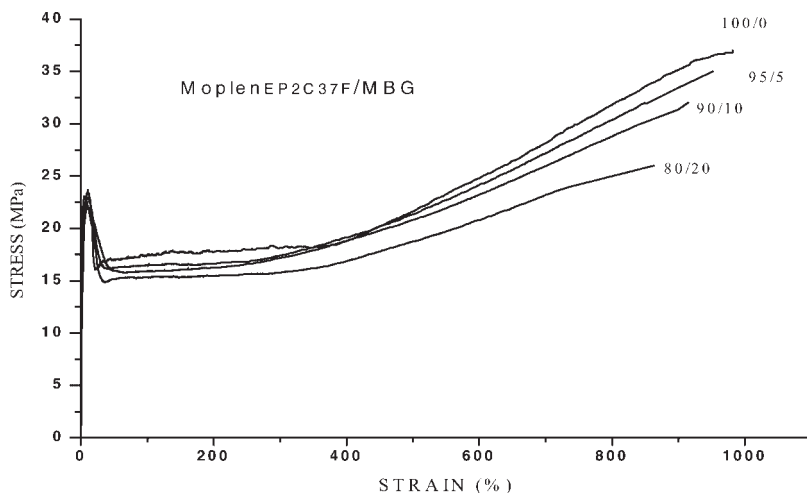


Figure 7. Stress-strain curves of MoplenEP2/MBG273 blends.

Table 4.

Tensile parameters of MoplenEP2/MBG273 blends at 25 °C.

MoplenEP2/MBG273 (wt/wt)	E (MPa)	ϵ_y (%)	σ_y (MPa)	ϵ_b (%)	σ_b (MPa)
100/0	1000 ± 66	10 ± 1	24 ± 1	981 ± 86	37 ± 1
95/5	1092 ± 115	10 ± 1	23 ± 1	952 ± 56	36 ± 1
90/10	1108 ± 101	10 ± 1	22 ± 1	915 ± 68	32 ± 1
80/20	1245 ± 119	5 ± 1	23 ± 1	862 ± 55	26 ± 2

hardening of the amorphous phase due to increase of Tg(L) contributes to increase it. The second effect is predominant over the first one and the overall balance is an increase of E.

Permeability

Table 5 reports water vapour permeability determined at 38 °C and at relative humidity of 90%. The results indicate that the addition of MBG273 to MoplenEP2 has the effect to decrease the water vapour permeability. For semicrystalline polymers the permeability value depends on two factors: the crystallinity fraction and the physical state of the amorphous phase. The crystalline phase is impermeable to gas and so the higher is the crystallinity fraction the lower is the permeability. The rubbery amorphous phase is more permeable to gas than the glassy amorphous phase, and so the harder is the amorphous phase the lower is the permeability. In the blends, the presence of MBG273 reduces the overall crystallinity of the material and, at the same time, changes gradually the amorphous phase from rubbery to glassy. The latter factor results predominant over the first one (reduction of crystallinity) and so

Table 5.

Permeability of MoplenEP2/MBG273 films and % decrease compared to MoplenEP2 film.

MoplenEP2/ MBG273 (wt/wt)	PERMEABILITY [ng/ (Pa · s · m)] · 10 ⁴	Decrease of permeability compared to MoplenEP2 film (%)
100/0	2.8 ± 0.1	–
95/5	2.2 ± 0.1	21
90/10	2.1 ± 0.1	25
80/20	1.7 ± 0.1	39

the water vapour permeability decreases with the resin content. It is relevant to observe that the addition of percentage of resins normally added to polyolefins, 5–10%, induces a percentage reduction of permeability over the 20%.

Conclusion

The hydrogenated hydrocarbon resin MBG273 is found to be compatible with the amorphous of a polypropylene copolymer, MoplenEP2C37F, up to the concentration used in this work, 20%. MoplenEP2/HR blends in the solid state form a two-phase system composed of a crystalline phase in α -monoclinic form and one amorphous phase. The hypothesis of the formation of only one amorphous phase is based on the analyses of Tg(L) measured by DSC and DMTA. With the addition of HR, Tg(L) increases from –6 °C for the MoplenEP2 to a value that for 80/20 blend is close to or higher than room temperature. This means that at ordinary temperature (about 25 °C) of use of these materials, the amorphous of the MoplenEP2 film, being in the rubbery state, has much higher mobility than the amorphous of the film derived from 80/20 blend. The addition of HR to MoplenEP2 makes the material harder. Stress-strain analysis shows that all the blends present curves similar to polypropylene material. In fact yielding point, cold-drawing and fibre-formation regions are formed also by 80/20 blend. The hardening of the blends with HR induces an enhancement Young's modulus and decrease of water vapour permeability over the 20%.

Acknowledgements: The authors warmly thank Mr. G. Loeber of Eastman Chemical Co. for supplying hydrogenated hydrocarbon resin MBG273 and helpful discussion about polyolefin/low-Mw-resin systems.

- [1] P. Buzio, B. Marcandalli, E. Martuscelli, A. Seves, *It. Pat.* 22196A **1990**.
- [2] S. Cimmino, P. Guarrata, E. Martuscelli, C. Silvestre, P. P. Buzio, *Polymer* **1991**, 32, 3299.
- [3] S. Cimmino, E. Di Pace, F. E. Karasz, E. Martuscelli, C. Silvestre, *Polymer* **1993**, 34, 972.
- [4] S. Cimmino, E. Martuscelli, C. Silvestre, *Die Makromolekulare Chemie, Macromol. Symp.* **1994**, 78, 115.
- [5] S. Cimmino, E. Di Pace, E. Martuscelli, L. C. Mendes, C. Silvestre, *J. Polym. Sci.* **1994**, 32, 2025.
- [6] S. Cimmino, E. Di Pace, E. Martuscelli, C. Silvestre, L. C. Mendes, G. Bonfanti, *J. Polym. Sci., Part B: Polym. Phys.* **1995**, 33, 1723.
- [7] E. Caponetti, D. Chillura Martino, S. Cimmino, M. A. Floriano, E. Martuscelli, C. Silvestre, R. Triolo, *J. Mol. Structure* **1996**, 383, 75.
- [8] C. Silvestre, S. Cimmino, E. Di Pace, M. L. Di Lorenzo, M. Monaco, *J. Macromol. Sci.-Phys.* **1996**, B 35, 457.
- [9] S. Cimmino, E. D'Alma, M.L. Di Lorenzo, E. Di Pace, C. Silvestre, *J. Polym. Sci.* **1999**, B 37, 867.
- [10] C. Silvestre, S. Cimmino, M.L. Di Lorenzo, *J. Appl. Polym. Sci.* **1999**, 71, 1677.
- [11] C. Silvestre, S. Cimmino, E. D'Alma, M.L. Di Lorenzo, E. Di Pace, *Polymer* **1999**, 40, 5119.
- [12] S. Cimmino, C. Silvestre, G. della Vecchia, *J. Appl. Polym. Sci.* **2004**, 92, 3465.
- [13] S. Cimmino, D. Duraccio, G. Loeber, C. Silvestre, paper in preparation.
- [14] K. Mezghani, P. Phillips, *Polymer* **1995**, 36 2407.
- [15] K. Mezghani, P. Phillips, *Polymer* **1997**, 38, 5725.
- [16] A. Dimiska, P. Phillips, 228 ACS National Meeting, Philadelphia, PA, USA, 2004, PMSE-337.
- [17] C. Silvestre, S. Cimmino, R. Triolo, *J. Poly. Sci: Part B: Polymer Phys.* **2003**, 41, 493.
- [18] J. Findlay, in: "Encyclopedia of Polymer Science and Engineering", H. F. Mark, N. M. Bikales, C. G. Overberger, G. Menges, J. I. Kroschwitz, Eds., **1987**, 9, 853.
- [19] S. Bruckner, S.V. Meille, V. Petraccone, B. Pirozzi, *Prog. Polym. Sci.* **1991**, 16, 361.
- [20] C. Silvestre, S. Cimmino, E. Di Pace, in: "Handbook of Polyolefins: Second Edition, Revised and Expanded" C. Vasile Ed., Marcell Dekker, chapter 7, pages 175–205, 2000.
- [21] A. Turner-Jones, J.M. Aizlewood, D.R. Beckett, *Macromolecular Chem.* **1964**, 75, 134.
- [22] A. Turner-Jones, *Polymer* **1971**, 12, 487.
- [23] R. F. Boyer, *J. Polym. Sci.* **1975**, 50, 189.
- [24] R. F. Boyer, *J. Macromol. Sci.- Phys.* **1973**, B8(3–4), 503.
- [25] P.H. Geil in: "Order in the amorphous state of polymers", S.E. Keinath, R.L. Miller, J.K. Rieke, Eds., **1987** Plenum Press, New York, p.83.
- [26] L. Beck, A.A. Hiltz, J.R. Knox, *SPE Trans.* **1963**, 3, 279.
- [27] M. Takayanagy, *Pure and Appl. Chem.* **1967**, 15, 555.
- [28] T. Nishi, T.T. Wang, *Macromolecules* **1975**, 8, 909.
- [29] K. Kwei, H.L. Frisch, *Macromolecules* **1978**, 11, 1267.